

Modal analysis of cracked cantilever composite beams

Murat Kisa†

Mechanical Engineering Department, Faculty of Engineering, Harran University, Sanliurfa, Turkey

M. Arif Gurel‡

Civil Engineering Department, Faculty of Engineering, Harran University, Sanliurfa, Turkey

(Received October 15, 2003, Accepted March 7, 2005)

Abstract. Modal analysis of cracked cantilever composite beams, made of graphite-fibre reinforced polyamide, is studied. By using the finite element and component mode synthesis methods, a numeric model applicable to investigate the vibration of cracked composite beams is developed. In this new approach, from the crack section, the composite beam separated into two parts coupled by a flexibility matrix taking into account the interaction forces. These forces are derived from the fracture mechanics theory as the inverse of the compliance matrix calculated with the proper stress intensity factors and strain energy release rate expressions. Numerical results are obtained for modal analysis of composite beams with a transverse non-propagating open crack, addressing the effects of the location and depth of the crack, and the volume fraction and orientation of the fibre on the natural frequencies and mode shapes. By means of modal data, the position and dimension of the defect can be found. The results of the study confirmed that presented method is suitable for the vibration analysis of cracked cantilever composite beams. Present technique can be easily extended to composite plates and shells.

Key words: composite; defects; damage assessment; numerical analysis; component mode synthesis.

1. Introduction

Advanced composite materials have been increasingly used over the past few decades as their high ratio of stiffness and strength to weight. During operation, all structures are subjected to degenerative effects that may trigger the initiation of structural defects such as cracks which, as time progresses, lead to the failure or collapse of the structure. As a consequence, the significance of examination in the quality assurance of manufactured products is well understood. Numerous techniques, such as non-destructive monitoring tests, can be used to screen the circumstance of a structure. Novel methods to examine structural defects such as cracks should be investigated. A crack in a structural element affects its dynamical performance and alters its stiffness and damping properties. Accordingly, the natural frequencies and mode shapes of the structure hold information concerning the location and size of the damage. Vibration analysis, which allows on line inspection, is an attractive method to detect cracks in the structures. What types of changes occur in the

† Doctor, Corresponding author, E-mail: mkisa@harran.edu.tr

‡ Doctor, E-mail: agurel@harran.edu.tr

vibration features, how these changes can be detected and how the condition of the structure is interpreted has been the topic of several research studies in the past (Cawley and Adams 1979, Gouranis and Dimarogonas 1988, Shen and Chu 1992, Ruotolo *et al.* 1996, Kisa *et al.* 1998, Kisa and Brandon 2000a, Kisa and Brandon 2000b) and reviewed by Wauer (1991) and Dimarogonas (1996).

Modal analysis of cracked composite beams has received a good amount of attention in the literature. Adams *et al.* (1978) showed that any defect in fibre reinforced plastics could be detected by reduction in natural frequencies and increase in damping. Nikpour and Dimarogonas (1988) investigated the variation of the mixed term in the energy release rate for various angles of inclination of the material axes of symmetry and derived the local compliance matrix of a prismatic beam having a central crack. Nikpour (1990) studied the buckling of cracked composite columns and showed that the instability increases with the column slenderness and the crack depth. Oral (1991) developed a shear flexible finite element for non-uniform laminated composite beams. He tested the performance of the element with isotropic and composite materials, constant and variable cross-sections, and straight and curved geometries. Krawczuk (1994) developed a new finite element for the static and dynamic analysis of cracked composite beams. He assumed that the crack changes only the stiffness of the element whereas the mass of the element is unchanged. Krawczuk and Ostachowicz (1995) investigated the eigenfrequencies of a cracked cantilever composite beam. They presented two models of the beam. In the first model the crack was modelled by a massless spring and in the second model the cracked part of the beam replaced by a cracked element. Krawczuk *et al.* (1997) proposed an algorithm to find the characteristic matrices of a composite beam with a single transverse fatigue crack. Recently, Song *et al.* (2003) investigated the dynamics of anisotropic composite cantilevers. He presented an exact solution methodology utilising Laplace transform technique to study the bending free vibration of cantilever composite beams with cracks.

The full eigensolution of a structure containing substructures each having large numbers of degrees of freedom can be cumbersome and costly in computing time. A method, which is called as 'substructuring', proposed by Hurty (1965) enabled the problem to be broken up into separate elements and thus considerably reduced its complexity. In many respects, the original rationale for such substructuring techniques has been rendered obsolete by the widespread availability of high performance computers. In this study the component mode synthesis method is used to separate a non-linear problem into two linear subsystems. To the authors' best knowledge this method is new and has not been used for the purposing of separating a global non-linear system into two linear subsystems, in the past studies.

2. Mathematical model

The model selected is a cantilever composite beam, of uniform cross section A , having a transverse edge crack of depth a at a variable position L_1 . The width, length and height of the beam are B , L and H , respectively, Fig. 1. The angle between the fibres and the axis of the beam is α .

The composite beam is partitioned into two components, A and B, at the crack section allowing to a substructure approach, Fig. 2. By separating the complete beam into two components, global non-linear system can be detached into two linear subsystems coupled by a local stiffness discontinuity. In the current study, every component is also divided into finite elements with two nodes and three degrees of freedom at each node as shown in Fig. 2.

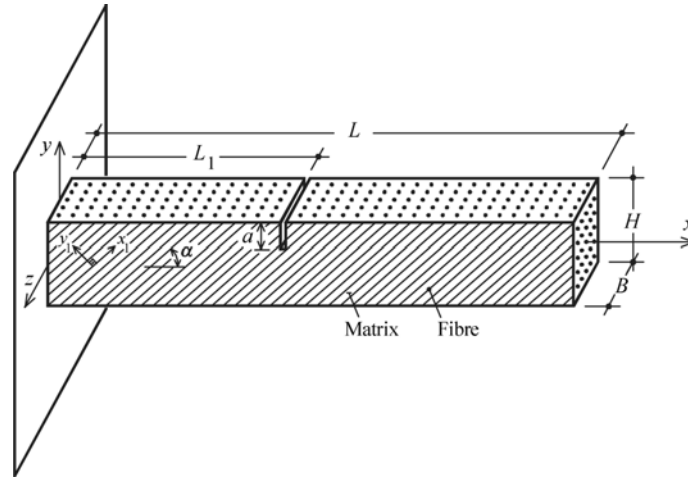


Fig. 1 Geometry of the cracked cantilever composite beam

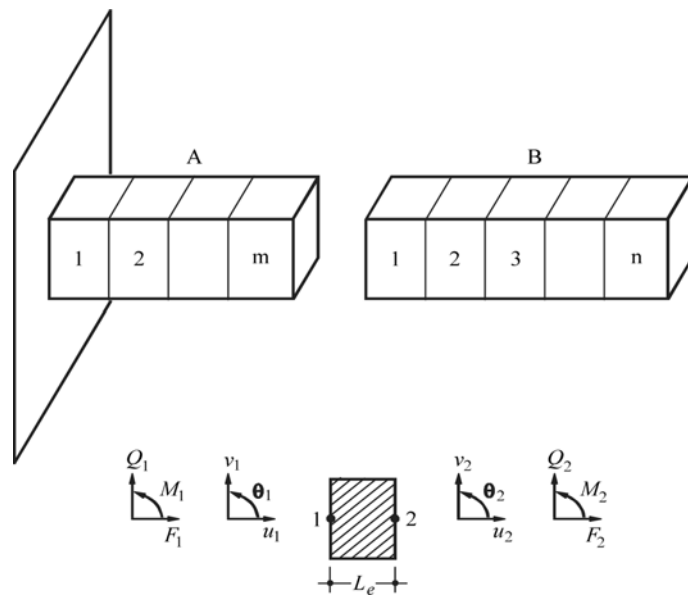


Fig. 2 Components of the whole structure and dividing them into the finite number of elements

2.1 Stiffness and mass matrices for composite beam element

The stiffness and mass matrices are developed from the procedure given by Krawczuk (1995) and modified to three degrees of freedom at each node, $\delta = \{u, v, \theta\}$. As can be seen in Fig. 2, representing a general finite element, the applied system forces, $F = \{F_1, Q_1, M_1, F_2, Q_2, M_2\}$, and the related displacements, $\delta = \{u_1, v_1, \theta_1, u_2, v_2, \theta_2\}$, are shown. The stiffness matrix for a two-noded composite beam element with three degrees of freedom $\delta = \{u, v, \theta\}$ at the each node, for bending in the xy plane, are given as follows

$$K_{el} = [k_{ij}]_{(6 \times 6)} \quad (1)$$

where k_{ij} ($i, j = 1, \dots, 6$) are given as

$$\begin{aligned} k_{11} &= k_{55} = 7BH\bar{S}_{33}/3L_e \\ k_{12} &= k_{21} = -k_{56} = -k_{65} = BH\bar{S}_{33}/2 \\ k_{13} &= k_{31} = k_{35} = k_{53} = -8BH\bar{S}_{33}/3L_e \\ k_{14} &= k_{41} = k_{36} = k_{63} = -k_{23} = -k_{32} = -k_{45} = -k_{54} = 2BH\bar{S}_{33}/3 \\ k_{15} &= k_{51} = BH\bar{S}_{33}/3L_e \\ k_{16} &= k_{61} = -k_{25} = -k_{52} = -BH\bar{S}_{33}/6 \\ k_{22} &= k_{66} = BH(7H^2\bar{S}_{11}/36L_e + L_e\bar{S}_{33}/9) \\ k_{24} &= k_{42} = k_{46} = k_{64} = BH(-2H^2\bar{S}_{11}/9L_e + L_e\bar{S}_{33}/9) \\ k_{26} &= k_{62} = BH(H^2\bar{S}_{11}/36L_e - L_e\bar{S}_{33}/18) \\ k_{33} &= 16BH\bar{S}_{33}/3L_e \\ k_{44} &= BH(4H^2\bar{S}_{11}/9L_e + 4L_e\bar{S}_{33}/9) \\ k_{34} &= k_{43} = 0 \end{aligned} \quad (2)$$

where B , H and L_e are the dimensions of the composite beam element. \bar{S}_{11} and \bar{S}_{33} are the stress-strain constants and given as, Vinson and Sierakowski (1991)

$$\bar{S}_{11} = S_{11}m^4 + 2(S_{12} + 2S_{33})m^2n^2 + S_{22}n^4 \quad (3)$$

$$\bar{S}_{33} = (S_{11} - 2S_{12} + S_{22} - 2S_{33})m^2n^2 + S_{33}(m^4 + n^4) \quad (4)$$

where $m = \cos \alpha$, $n = \sin \alpha$ and S_{ij} terms are determined from the relations

$$S_{11} = \frac{E_{11}}{(1 - \nu_{12}^2 E_{22}/E_{11})}, \quad S_{22} = S_{11}E_{22}/E_{11}, \quad S_{12} = \nu_{12}S_{22}, \quad S_{33} = G_{12} \quad (5)$$

where E_{11} , E_{22} , G_{12} , and ν_{12} are the mechanical properties of the composite and can be determined as shown in the Appendix.

The mass matrix of the composite beam element can be given as

$$M_{el} = [m_{ij}]_{(6 \times 6)} \quad (6)$$

where m_{ij} ($i, j = 1, \dots, 6$) are

$$\begin{aligned} m_{11} &= m_{55} = 2\rho BHL_e/15 \\ m_{12} &= m_{21} = -m_{56} = -m_{65} = \rho BHL_e^2/180 \end{aligned}$$

$$\begin{aligned}
 m_{13} &= m_{31} = m_{35} = m_{53} = \rho B H L_e / 15 \\
 m_{14} &= m_{41} = -m_{45} = -m_{54} = -\rho B H L_e^2 / 90 \\
 m_{36} &= m_{63} = m_{23} = m_{32} = m_{34} = m_{43} = 0 \\
 m_{15} &= m_{51} = -\rho B H L_e / 30 \\
 m_{16} &= m_{61} = -m_{25} = -m_{52} = \rho B H L_e^2 / 180 \\
 m_{22} &= m_{66} = \rho B H L_e (L_e^2 / 1890 - H^2 / 360) \\
 m_{24} &= m_{42} = m_{46} = m_{64} = \rho B H L_e (-L_e^2 / 945 + H^2 / 180) \\
 m_{26} &= m_{62} = \rho B H L_e (L_e^2 / 1890 - H^2 / 360) \\
 m_{33} &= 8 \rho B H L_e / 15 \\
 m_{44} &= \rho B H L_e (2 L_e^2 / 945 + 2 H^2 / 45)
 \end{aligned} \tag{7}$$

where ρ is the mass density of the element.

2.2 The stiffness matrix induced by the crack

According to the St Venant's principle, the stress field is influenced only in the region near to the crack. The additional strain energy due to crack leads to flexibility coefficients expressed by stress intensity factors derived by means of Castigliano's theorem in the linear elastic range. The compliance coefficients C_{ij} induced by the crack are derived from the strain energy release rate, J , developed in Griffith-Irwin theory (Tada *et al.* 1985). J can be given as

$$J = \frac{\partial U(P_i, A)}{\partial A} \tag{8}$$

where A is the area of the crack section, P_i are the corresponding loads, U is the strain energy of the beam due to crack and can be expressed as, Nikpour and Dimarogonas (1988)

$$U = \int_A \left(D_1 \sum_{i=1}^{i=N} K_{Ii}^2 + D_{12} \sum_{i=1}^{i=N} K_{Ii} \sum_{j=1}^{j=N} K_{IIj} + D_2 \sum_{i=1}^{i=N} K_{IIi}^2 \right) dA \tag{9}$$

where K_I and K_{II} are the stress intensity factors for the fracture modes of *I* and *II*. Coefficients D_1 , D_{12} and D_2 are depending on the materials parameters

$$D_1 = -0.5 \bar{b}_{22} \text{Im} \left(\frac{s_1 + s_2}{s_1 s_2} \right) \tag{10}$$

$$D_{12} = \bar{b}_{11} \text{Im}(s_1 s_2) \tag{11}$$

$$D_2 = 0.5 \bar{b}_{11} \text{Im}(s_1 + s_2) \tag{12}$$

The coefficients s_1 , s_2 and \bar{b}_{ij} are given in the Appendix. The mode *I* and *II* stress intensity factors, K_I and K_{II} , for a composite beam with a crack are expressed as, Bao *et al.* (1992)

$$K_{ji} = \sigma_i \sqrt{\pi a} Y_j(\xi) F_{ji}(a/H) \quad (13)$$

where σ_i is the stress for the corresponding fracture mode, $F_{ji}(a/H)$ is the correction factor for the finite specimen size, $Y_j(\xi)$ is the correction factor for the anisotropic material, a is the crack depth and H is the element height. Castigliano's theorem (Przemieniecki 1967) implies that the additional displacement due to crack, according to the direction of the P_i , is

$$u_i = \frac{\partial U(P_i, A)}{\partial P_i} \quad (14)$$

Substituting the strain energy release rate J into Eq. (14) the relation between displacement and strain energy release rate J can be written as follows

$$u_i = \frac{\partial}{\partial P_i} \int J(P_i, A) dA \quad (15)$$

The flexibility coefficients, which are the functions of the crack shape and the stress intensity factors, can be introduced as follows

$$c_{ij} = \frac{\partial u_i}{\partial P_j} = \frac{\partial^2}{\partial P_i \partial P_j} \int J(P_i, A) dA = \frac{\partial^2 U}{\partial P_i \partial P_j} \quad (16)$$

The compliance coefficients matrix, after being derived from above equation, can be given according to the displacement vector $\delta = \{u, v, \theta\}$ as

$$C = [c_{ij}]_{(3 \times 3)} \quad (17)$$

where $c_{ij}(i, j = 1, 2, 3)$ are derived by using Eqs. (8) to (16).

The inverse of the compliance coefficients matrix, C^{-1} , is the stiffness matrix due to crack. Considering the cracked node as a cracked element of zero length and zero mass, the crack stiffness matrix can be represented by equivalent compliance coefficients. Finally, resulting stiffness matrix for the crack can be given as

$$K_c = \begin{bmatrix} [C]^{-1} & -[C]^{-1} \\ [C]^{-1} & [C]^{-1} \end{bmatrix}_{(6 \times 6)} \quad (18)$$

3. Component mode synthesis

The equation of motion of a mid-plane symmetrical composite beam is, Vinson and Sierakowski (1991)

$$IS_{11} \partial^4 y(x, t) / \partial x^4 + \rho A \partial^2 y(x, t) / \partial t^2 = f(t) \quad (19)$$

where I , ρ , A , $y(x, t)$ and $f(t)$ are the geometrical moment of inertia of the beam cross-section, material density, cross-sectional area of the beam, transverse deflection of the beam and the global force vector for the system, respectively. Now, consider the component A, Fig. 2, for undamped free vibration analysis, the equation of motion can be given as

$$I\ddot{s}_A + \omega_A^2 s_A = \psi_A^T f_A(t) \quad (20)$$

where I , s_A , ψ_A^T and ω_A^2 are the identity matrix, principal modal coordinates, mass normalised mode vector and a diagonal matrix comprising the eigenvalues of A, respectively.

3.1 Coupling of the components

If two components, A and B, are connected together by spring, as shown in Fig. 3, then the kinetic and strain energy of the two components, in terms of principal modal coordinates, can be given as

$$\begin{aligned} T &= \frac{1}{2} \dot{s}^T M \dot{s} \\ U &= \frac{1}{2} s^T K s \end{aligned} \quad (21)$$

where T and U are kinetic and strain energy, respectively. M and K in Eq. (21) are

$$M = \begin{bmatrix} I & 0 \\ 0 & I \end{bmatrix} \quad K = \begin{bmatrix} \omega_A^2 & 0 \\ 0 & \omega_B^2 \end{bmatrix} \quad (22)$$

The strain energy of the connectors, in terms of principal modal coordinates, is

$$U_C = \frac{1}{2} s^T \psi^T K_C \psi s \quad (23)$$

where K_C is the stiffness matrix of the cracked nodal element and can be calculated by using Eq. (18). ψ in Eq. (23) can be written as

$$\psi = \begin{bmatrix} \psi_A & 0 \\ 0 & \psi_B \end{bmatrix} \quad (24)$$

The total strain energy of the system is, therefore,

$$U_T = \frac{1}{2} s^T (K + \psi^T K_C \psi) s \quad (25)$$

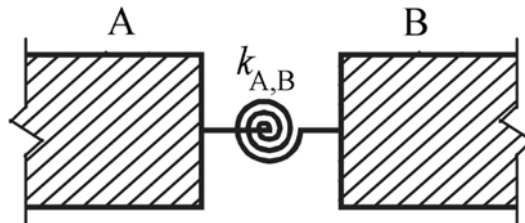


Fig. 3 Two components connected by spring

where K has been given by Eq. (22). The equation of motion of the complete structure is

$$\ddot{s}(K + \psi^T K_C \psi)s = \psi^T f(t) \quad (26)$$

where ψ has been given by Eq. (24). From Eq. (26), which is solved by the Lanczos algorithm, the eigenvalues and eigenvectors of the cracked system can be determined.

4. Numerical examples and discussion

4.1 Uniform cantilever composite beam

As a first example, the uniform cantilever composite beam with a transverse non-propagating open crack, shown in Fig. 1, is chosen and the described method has been applied. The beam assumed to be made of unidirectional graphite fibre-reinforced polyamide. In order to check the accuracy of the model the geometrical characteristics and material properties of the beam were chosen as the same of those used by Krawczuk *et al.* (1997). The material properties of the graphite fibre-reinforced polyamide composite, in terms of fibres and matrix, identified by the indices f and m , respectively, are

Modulus of Elasticity	: $E_m = 2.756$ GPa, $E_f = 275.6$ GPa
Modulus of Rigidity	: $G_m = 1.036$ GPa, $G_f = 114.8$ GPa
Poisson's Ratio	: $\nu_m = 0.33$, $\nu_f = 0.2$
Mass Density	: $\rho_m = 1600$ kg/m ³ , $\rho_f = 1900$ kg/m ³

The geometrical characteristics, the length (L), height (H) and width (B) of the composite beam, as consistent with those used by Krawczuk *et al.* (1997), are chosen as 0.6 m, 0.025 m and 0.05 m, respectively.

Firstly, the presented method has been applied for the free vibration analysis of corresponding non-cracked composite cantilever beam. The three lowest eigenfrequencies for various values of the angle of the fibre (α) and the volume fraction of fibre (V) are determined. As shown in Fig. 4, the results that found by using a four element model are compared with the analytical and numerical solutions found in the literature (Krawczuk *et al.* 1997, Vinson and Sierakowski 1991). The non-dimensional natural frequencies are normalised according to the following relation

$$\bar{\omega}_i = L\sqrt{\omega_i H / \sqrt{S_{11}} / 12\rho} \quad (27)$$

where L , H and ω_i show the length, height of the beam and the i th dimensional natural frequency, respectively. As can be seen from the Figures, an excellent agreement has been found between the results.

Secondly, the natural frequencies and mode shapes of the cracked cantilever composite beam are analysed. The calculations have been carried out for various volume fractions of the fibre (V), the fibre angles (α) and the crack ratios (a/H). The natural frequencies of the cracked cantilever composite beam are lower than those of the corresponding intact beam, as expected. In Fig. 5, the changes in the first natural frequency of the cracked beam are given as a function of the different

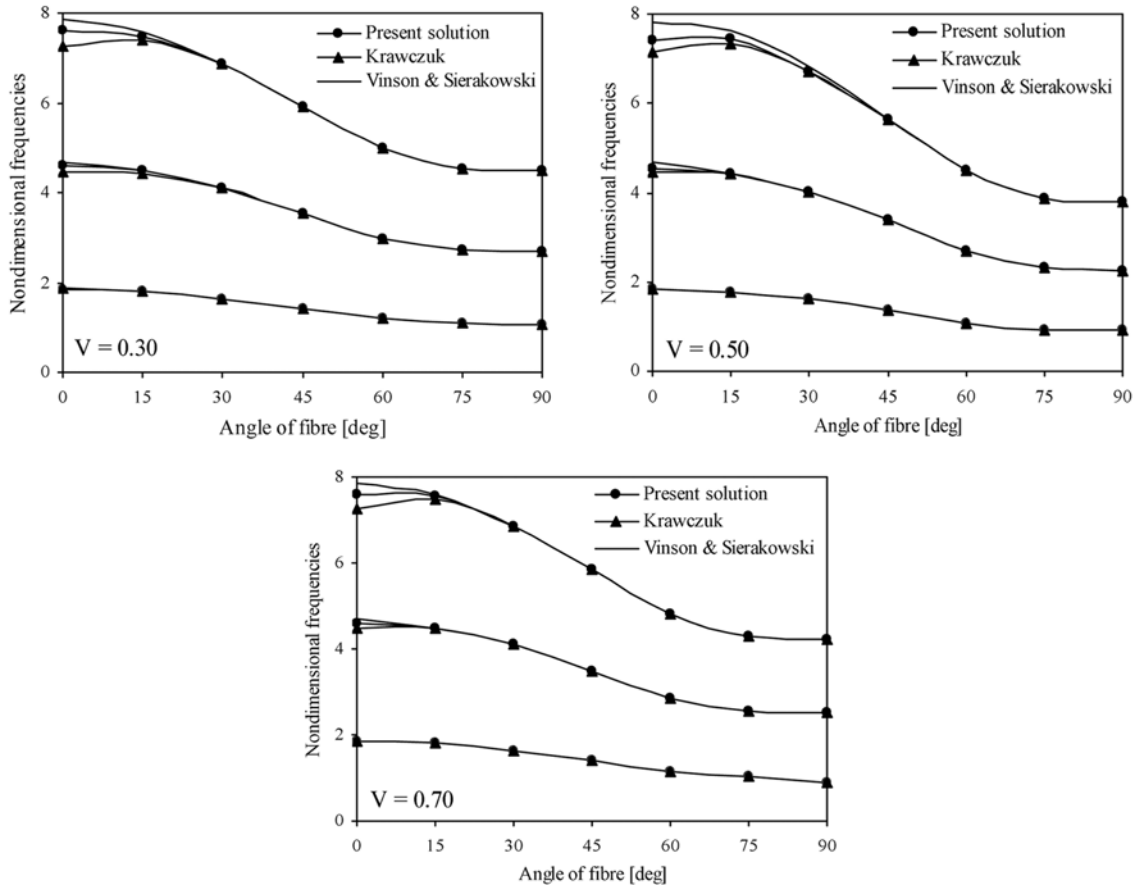


Fig. 4 Non-dimensional natural frequencies of the intact composite beam as a function of the fibre angle α , for various volume fractions V

crack ratios (a/H) and the fibre orientations (α) for several volume fractions of fibre (V). First non-dimensional natural frequencies are normalised according to following equation

$$\omega = \frac{\omega(\alpha)}{\omega_{nc}(\alpha)} \tag{28}$$

where $\omega(\alpha)$ and $\omega_{nc}(\alpha)$ denote the first natural frequency of the cracked and non-cracked cantilever composite beam as a function of the angle of the fibre (α), respectively.

As seen in Fig. 5, when the crack is perpendicular to the fibre direction ($\alpha = 0^\circ$), the decrease in the first natural frequency is the highest. As the angle of the fibre increases, the changes in the first frequency reduce. For the value of the angle of fibre is greater than 45° these changes are very low and the cracked cantilever composite beam behaves as if a non-cracked beam. This can be explained as the flexibility due to crack is negligible when the angle of the fibre is greater than 45° (Krawczuk *et al.* 1997). The flexibility induced by the crack is higher when the volume fraction of the fibre is between 0.2 and 0.8 (Krawczuk *et al.* 1997), and the maximum when $V = 0.45$. This can

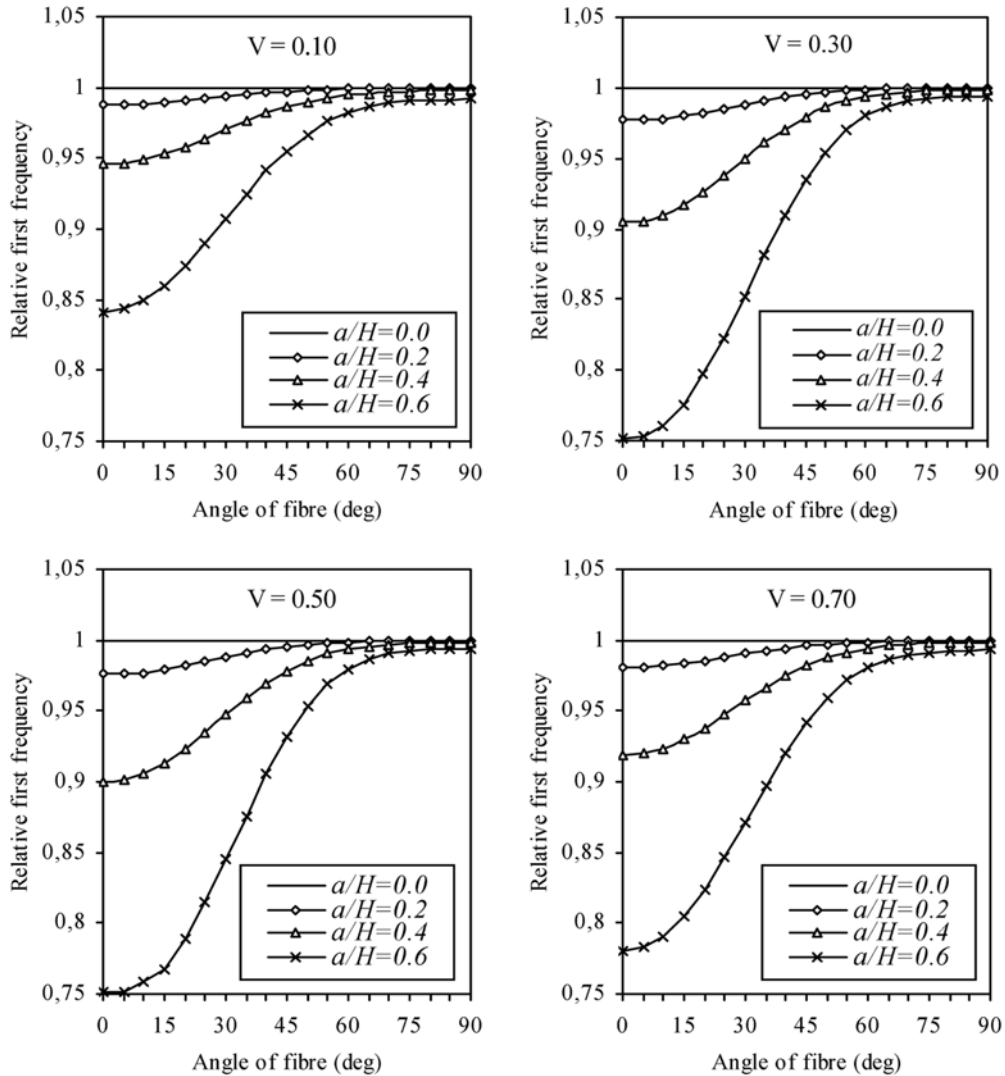


Fig. 5 Changes in the first natural frequency of the cracked composite beam as a function of the angle of the fibre α , for various crack ratios a/H and volume fractions V

be clearly seen from Fig. 5, as the reduction in the first natural frequency is higher for the volume fraction of the fibre is between 0.3 and 0.5.

In Fig. 6, the variation of the first natural frequencies of the cracked cantilever composite beam is presented as a function of relative crack positions (L_1/L) and depths (a/H). In the analysis, the volume fraction and angle of fibre are assumed to be 0.1 and 0° , respectively. Non-dimensional natural frequencies are normalised according to Eq. (28). Due to the bending moment along the beam, which is concentrated at the fixed end, a crack near the free end will have a smaller effect on the fundamental frequency than a crack closer to the fixed end, and as seen from Fig. 6, it can be concluded that the frequencies are almost unchanged when the crack is located away from the fixed end.

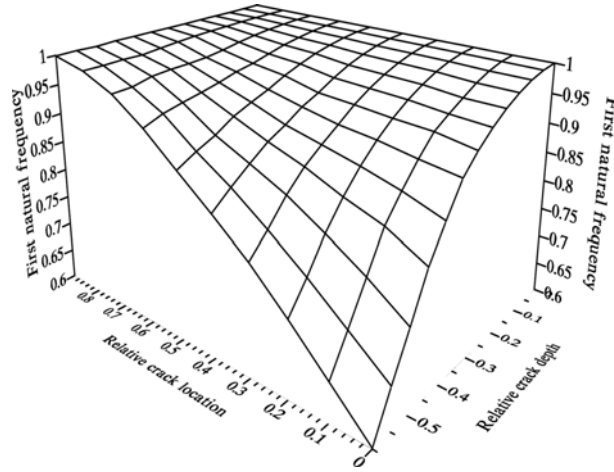


Fig. 6 Changes in the first natural frequency for various relative crack depth and location

In Figs. 7, 8 and 9, the first, second and third natural bending mode shapes of the cracked cantilever composite beam for the values of the angle of fibre $\alpha = 0^\circ, 30^\circ, 60^\circ$ and 90° are shown. The mode shapes have been found by assuming that the crack location (L_1/L), volume fraction of fibre (V) and crack ratio (a/H) are equal to 0.1, 0.1 and 0.2, respectively. The mode shapes show that the effect of the angle of the fibre is the highest when $\alpha = 0^\circ$. As the fibre angle increases, the changes in the mode shape decrease. If the angle of the fibre is greater than 45° , while the first and second natural bending mode shapes do not give much information about the defect, the third

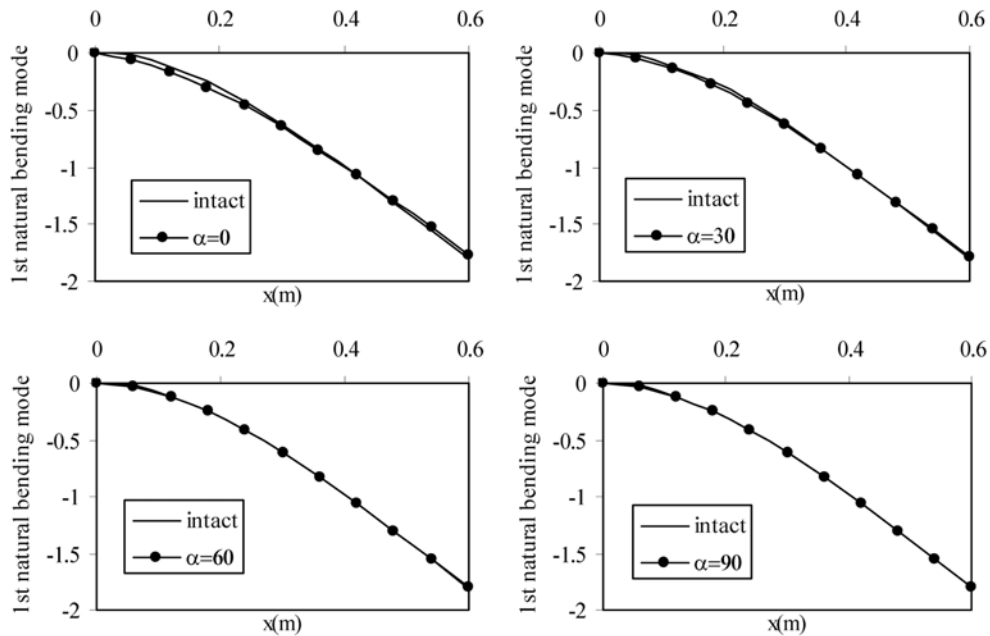


Fig. 7 First natural bending mode shapes of the cracked composite beam for the values of the angle of fibres $\alpha = 0^\circ, 30^\circ, 60^\circ, 90^\circ$ and $L_1/L = 0.1, V = 0.1, a/H = 0.2$

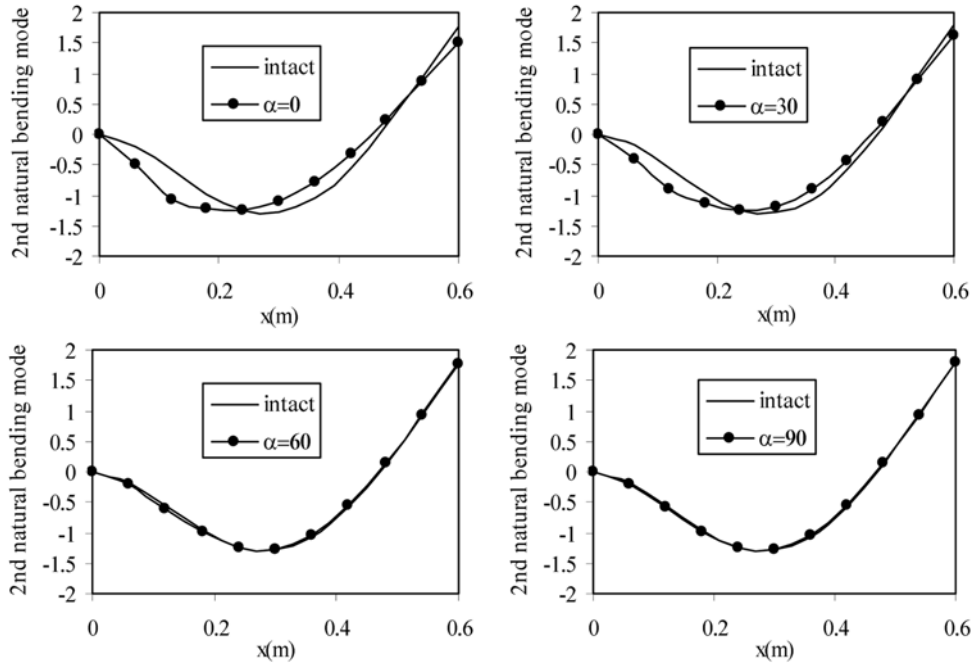


Fig. 8 Second natural bending mode shapes of the cracked composite beam for the values of the angle of fibres $\alpha = 0^\circ, 30^\circ, 60^\circ, 90^\circ$ and $L_1/L = 0.1, V = 0.1, a/H = 0.2$

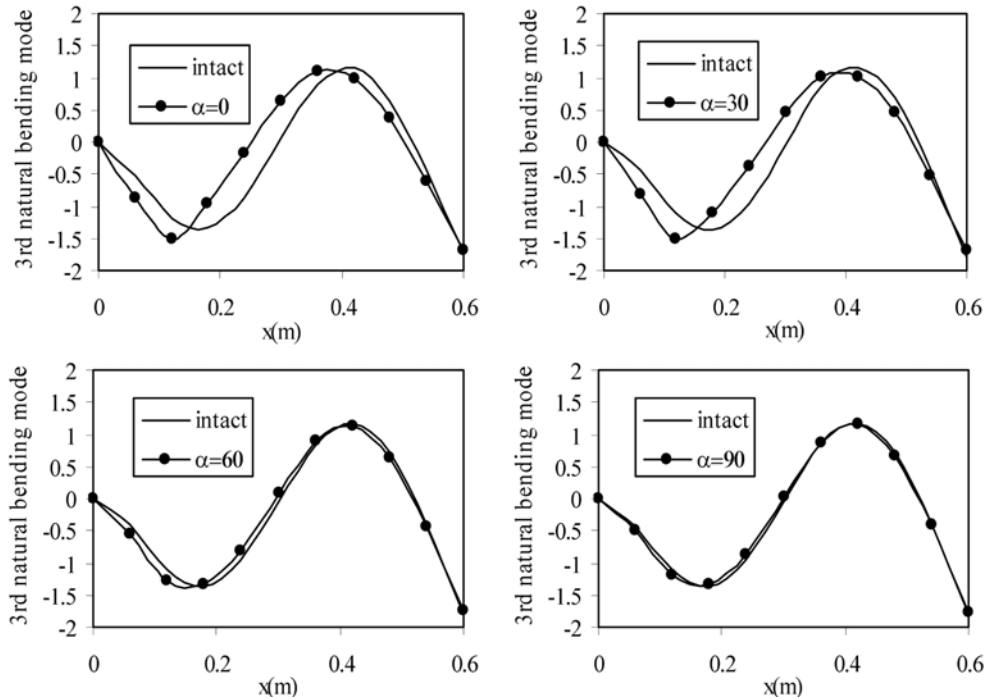


Fig. 9 Third natural bending mode shapes of the cracked composite beam for the values of the angle of fibres $\alpha = 0^\circ, 30^\circ, 60^\circ, 90^\circ$ and $L_1/L = 0.1, V = 0.1, a/H = 0.2$

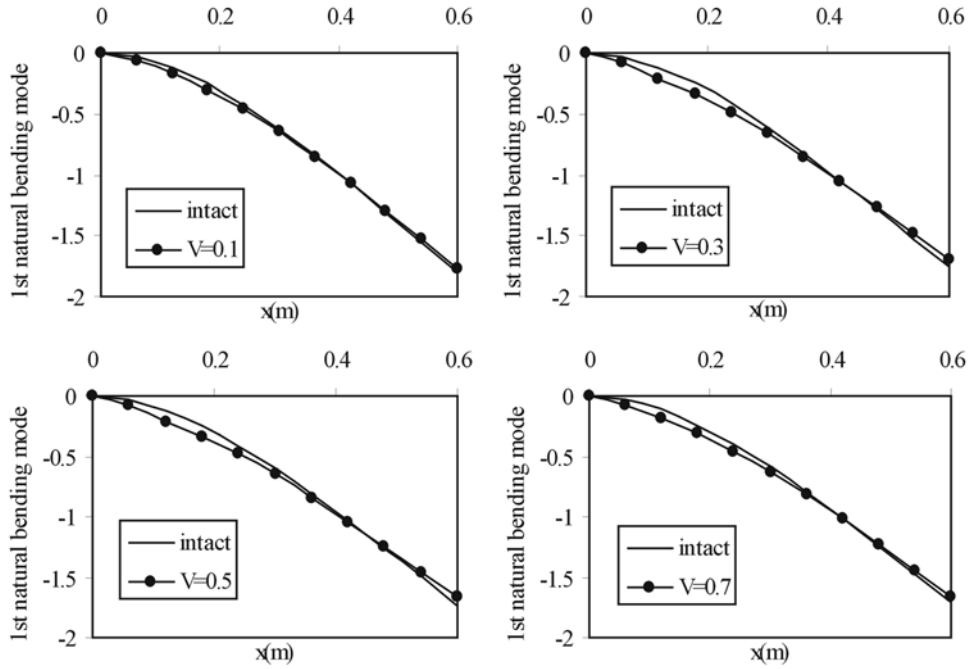


Fig. 10 First natural bending mode shapes of the cracked composite beam for the values of the volume fraction of fibre $V = 0.1, 0.3, 0.5, 0.7$ and $L_1/L = 0.1, \alpha = 0^\circ, a/H = 0.2$

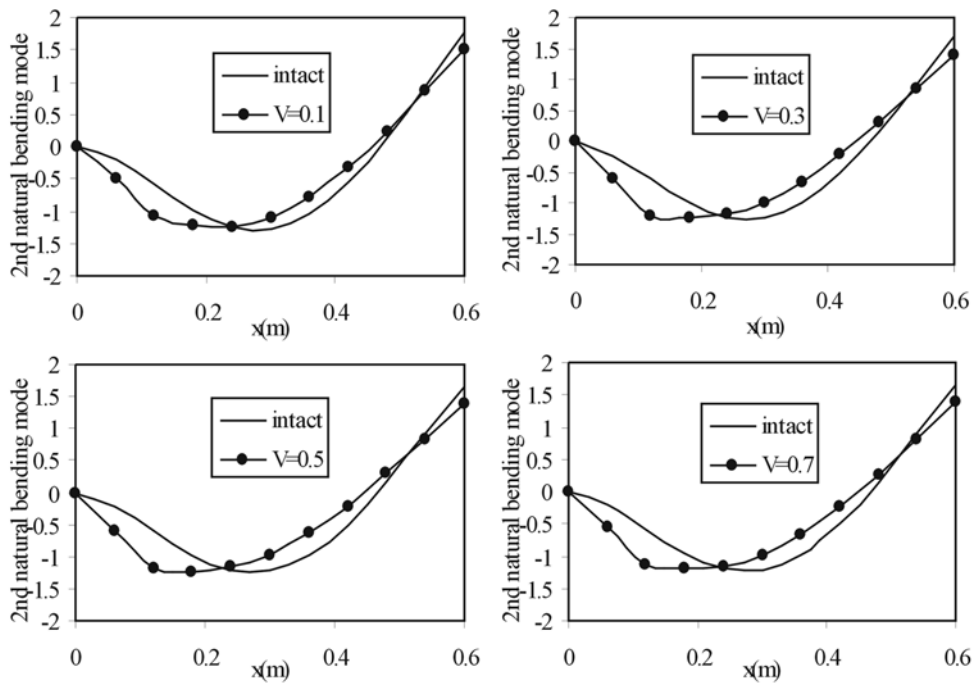


Fig. 11 Second natural bending mode shapes of the cracked composite beam for the values of the volume fraction of fibre $V = 0.1, 0.3, 0.5, 0.7$ and $L_1/L = 0.1, \alpha = 0^\circ, a/H = 0.2$

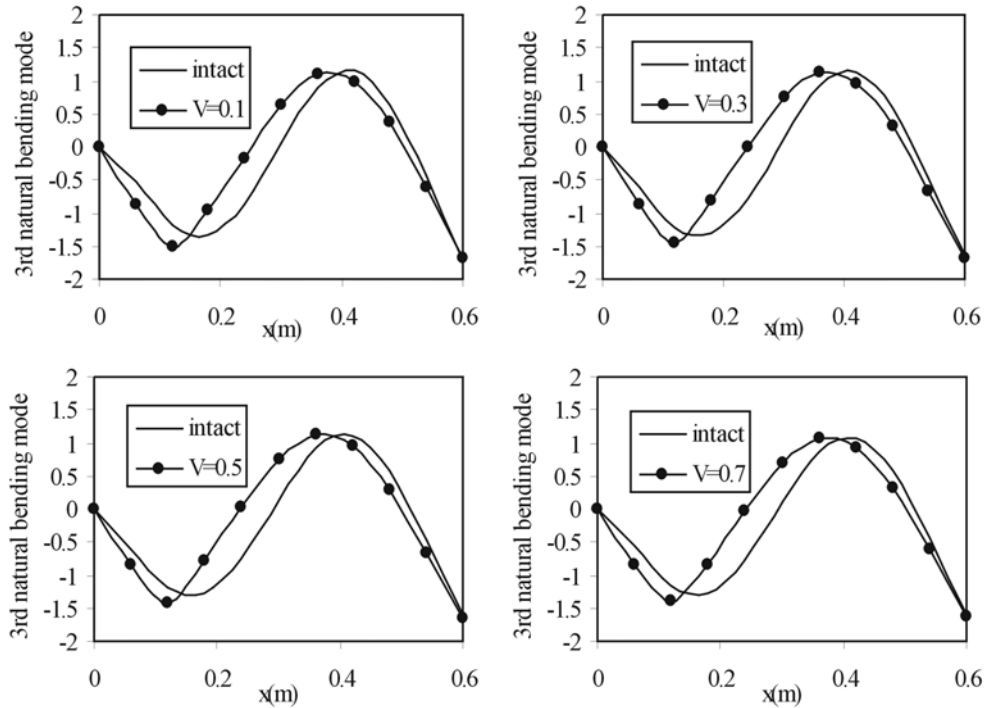


Fig. 12 Third natural bending mode shapes of the cracked composite beam for the values of the volume fraction of fibre $V = 0.1, 0.3, 0.5, 0.7$ and $L_1/L = 0.1$, $\alpha = 0^\circ$, $a/H = 0.2$

natural bending mode shape, as can be seen in Fig. 9, contains more information about the crack. Consequently for the inspection of the structures, several mode shapes should be investigated.

Figs. 10, 11 and 12 show the first, second and third natural bending mode shapes of the cracked cantilever composite beam for the values of the volume fraction of fibre $V = 0.1, 0.3, 0.5$ and 0.7 . In the analysis, crack location (L_1/L), angle of fibre (α) and crack ratio (a/H) are taken as 0.1 , 0° and 0.2 , respectively. From the figures, it is clearly seen that the changes in the first, second and third natural bending mode shapes are higher for the volume fraction of the fibre is between 0.2 and 0.8 .

4.2 Two-step cantilever composite beam

Second example is chosen as a two-step cracked cantilever composite beam shown in Fig. 13. The material properties of the composite beam are identical to the beam in the preceding example and the geometrical properties are $L_1 = 0.36$ m, $L_2 = 0.24$ m, $H_1 = 0.025$ m, $H_2 = 0.02$ m and $B = 0.05$ m.

In Fig. 14, the variation of the first natural frequencies of the two-step cracked composite beam is presented as a function of relative crack positions (L_c/L) and depths (a/H).

In the analysis, the volume fraction and angle of fibre are assumed to be 0.1 and 0° , respectively. Non-dimensional natural frequencies are normalised according to Eq. (28). As seen from the figure, a crack near the fixed end has greater effects on the fundamental frequency. The location of the change of cross-section of the beam can be clearly discerned from the figure.

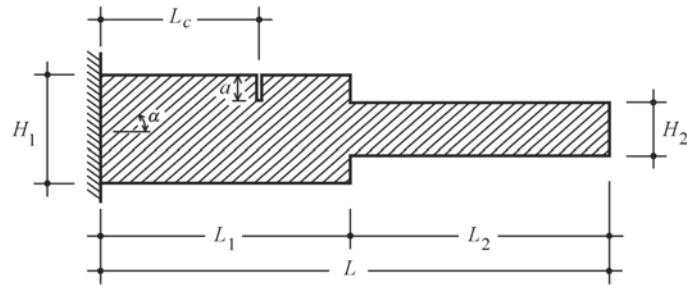


Fig. 13 Geometry of the stepped composite beam

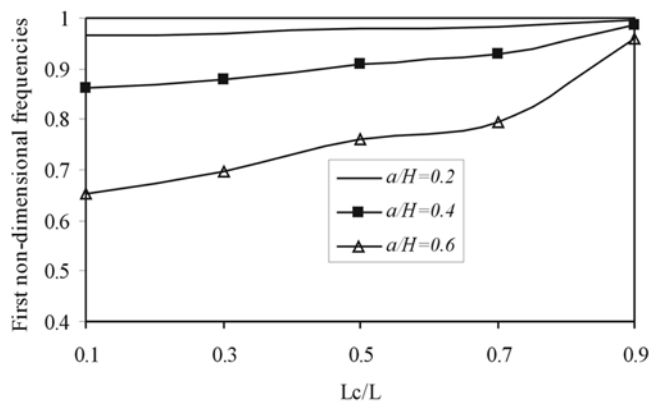


Fig. 14 First non-dimensional natural bending frequencies as a function of crack location for various crack ratios, when $V = 0.1$ and $\alpha = 0^\circ$

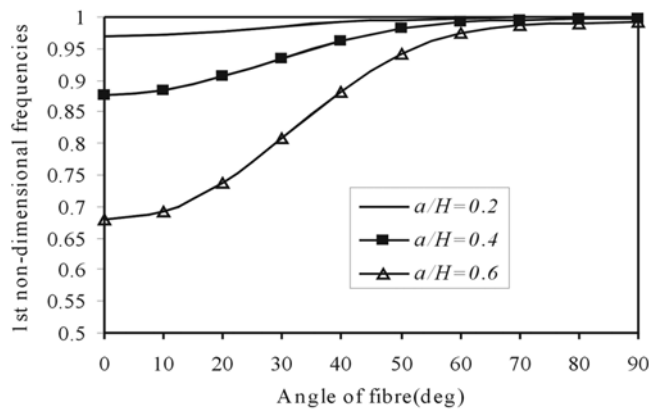


Fig. 15 First non-dimensional natural bending frequencies as a function of the angle of fibre for various crack ratios, when $L_c/L = 0.1$ and $V = 0.1$

In Fig. 15, by assuming that $L_c/L = 0.1$ and $V = 0.1$, the changes in the first natural bending frequency of the two-step cracked beam are given as a function of the fibre orientations (α), for several crack ratios (a/H). Again, it is obvious that, as the flexibility due to crack is maximum when

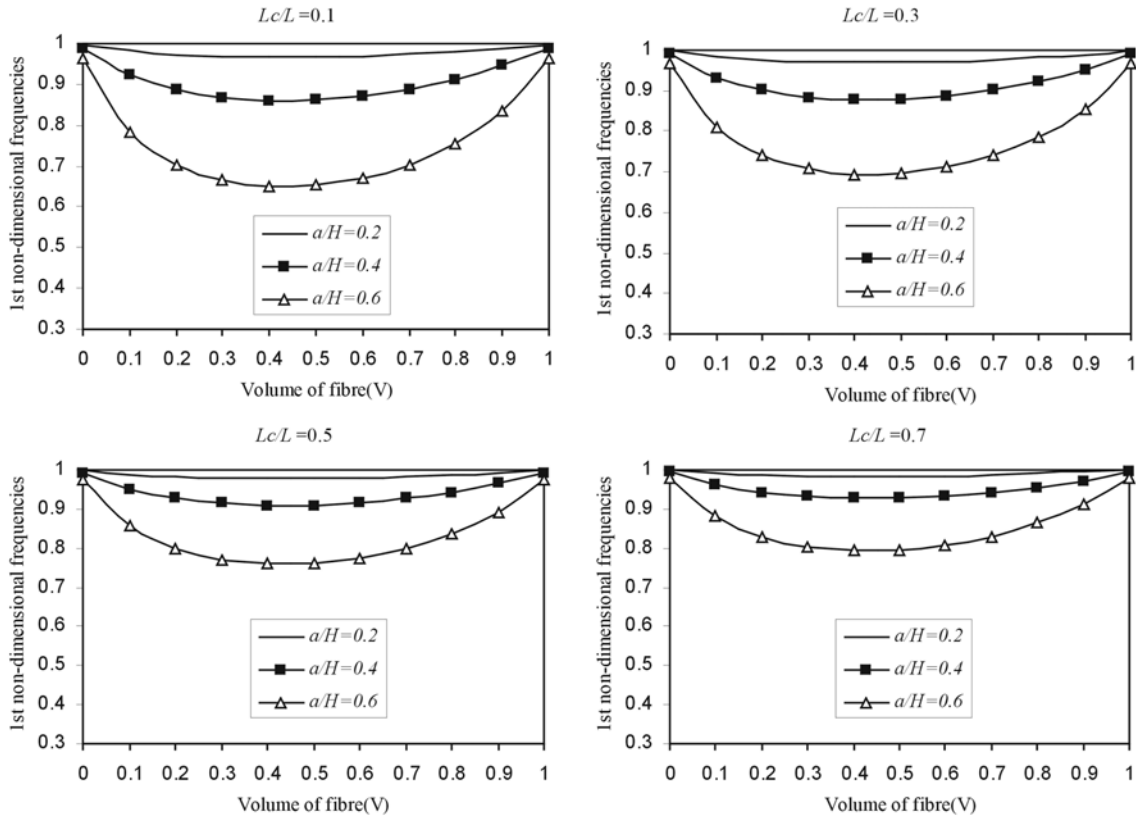


Fig. 16 Changes in the first non-dimensional natural bending frequencies as a function of the volume fraction of fibre for various crack ratios and locations

the angle of the fibre is equal to 0° (Krawczuk *et al.* 1997), when the crack is perpendicular to the fibre direction, the decrease in the first natural frequency is the highest.

As discussed in the first example, the flexibility induced by the crack is higher when the volume fraction of the fibre is between 0.2 and 0.8, and maximum when $V = 0.45$. This can be apparently seen from the Fig. 16 that illustrates the changes in the first non-dimensional natural bending frequencies as a function of the volume fraction of fibre for various crack ratios and locations.

5. Conclusions

In this paper a new approach for the modal analysis of cracked composite beams has been presented. It is showed that the knowledge of modal data of cracked composite beams forms an important aspect in assessing the structural failure. It is noted that if the angle of the fibre is greater than 45° , as the first and second natural bending mode shapes do not contain much information about the defect; several mode shapes should be examined. To illustrate the effectiveness of the approach, results have been compared with previous studies published in the literature leading to confidence in the validity of this approach. In the method, the component mode synthesis technique

is used and a non-linear problem divided into two linear subsystems. As the whole structure is separated from the crack section, present approach is capable of analysing the non-linear interface effects such as contact and impact that occur when crack closes.

It is evident that, the analysis of the present study is mainly for cantilever composite beams with constant or abruptly changing cross-sections. However, extension to tapered cantilever beams can be carried out trivially. Other possible extensions of the present study are the investigation of the beams with other boundary conditions, inclusion of damping to the analysis and consideration of the propagating of crack, which are left for future works.

References

- Adams, R.D., Cawley, P., Pye, C.J. and Stone, J. (1978), "A vibration testing for non-destructively assessing the integrity of the structures", *J. Mech. Eng. Sci.*, **20**, 93-100.
- Bao, G., Ho, S., Suo, Z. and Fan, B. (1992), "The role of material orthotropy in fracture specimens for composites", *Int. J. Solids Struct.*, **29**, 1105-1116.
- Cawley, P. and Adams, R.D. (1979), "The location of defects in structures from measurements of natural frequencies", *J. Strain Analysis*, **14**, 49-57.
- Dimarogonas, A.D. (1996), "Vibration of cracked structures: A state of the art review", *Eng. Fract. Mech.*, **55**(5), 831-857.
- Gouranis, G. and Dimarogonas, A.D. (1988), "A finite element of a cracked prismatic beam for structural analysis", *Comput. Struct.*, **28**, 309-313.
- Hurty, W.C. (1965), "Dynamic analysis of structures using substructure modes", *AIAA J.*, **3**, 678-685.
- Kisa, M., Brandon, J.A. and Topcu, M. (1998), "Free vibration analysis of cracked beams by a combination of finite elements and component mode synthesis methods", *Comput. Struct.*, **67**(4), 215-223.
- Kisa, M. and Brandon, J.A. (2000a), "Free vibration analysis of multiple open-edge cracked beams by component mode synthesis", *Struct. Eng. Mech.*, **10**(1), 81-92.
- Kisa, M. and Brandon, J.A. (2000b), "The effects of closure of cracks on the dynamics of a cracked cantilever beam", *J. Sound Vib.*, **238**(1), 1-18.
- Krawczuk, M., Ostachowicz, W. and Zak, A. (1997), "Modal analysis of cracked, unidirectional composite beam", *Composites Part B*, **28B**, 641-650.
- Krawczuk, M. and Ostachowicz, W.M. (1995), "Modelling and vibration analysis of a cantilever composite beam with a transverse open crack", *J. Sound Vib.*, **183**(1), 69-89.
- Krawczuk, M. (1994), "A new finite element for the static and dynamic analysis of cracked composite beams", *Comput. Struct.*, **52**(3), 551-561.
- Nikpour, K. and Dimarogonas, A.D. (1988), "Local compliance of composite cracked bodies". *Compos. Sci. Technol.*, **32**, 209-223.
- Nikpour, K. (1990), "Buckling of cracked composite columns", *Int. J. Solids Struct.*, **26**(12), 1371-1386.
- Oral, S. (1991), "A shear flexible finite element for non-uniform laminated composite beams", *Comput. Struct.*, **38**(3), 353-360.
- Przemieniecki, J.S. (1967), *Theory of Matrix Structural Analysis*, London, McGraw-Hill, first edition.
- Ruotolo, R., Surace, C., Crespo, P. and Storer, D. (1996), "Harmonic analysis of the vibrations of a cantilevered beam with a closing crack", *Comput. Struct.*, **61**, 1057-1074.
- Shen, M.H.H. and Chu, Y.C. (1992), "Vibrations of beams with a fatigue crack", *Comput. Struct.*, **45**, 79-93.
- Song, O., Ha, T.W. and Librescu, L. (2003), "Dynamics of anisotropic composite cantilevers weakened by multiple transverse open cracks", *Eng. Fract. Mech.*, **70**, 105-123.
- Tada, H., Paris, P.C. and Irwin, G.R. (1985), *The Stress Analysis of Cracks Handbook*, St. Louis, Missouri 63105, Paris production incorporated and Del Research Corporation, Second edition.
- Vinson, J.R. and Sierakowski, R.L. (1991), *Behaviour of Structures Composed of Composite Materials*, Dordrecht, Martinus Nijhoff, first edition.
- Wauer, J. (1991), "Dynamics of cracked rotors: a literature survey", *Applied Mechanics Reviews*, **17**, 1-7.

Appendix

The roots of following characteristic equation give the complex constans s_1 and s_2 (Vinson and Sierakowski 1991)

$$\bar{b}_{11}s^4 - 2\bar{b}_{16}s^3 + (2\bar{b}_{12} + \bar{b}_{66})s^2 - 2\bar{b}_{26}s + \bar{b}_{22} = 0$$

where \bar{b}_{ij} constans are

$$\bar{b}_{11} = b_{11}m^4 + (2b_{12} + b_{66})m^2n^2 + b_{22}n^4$$

$$\bar{b}_{22} = b_{11}n^4 + (2b_{12} + b_{66})m^2n^2 + b_{22}m^4$$

$$\bar{b}_{12} = (b_{11} + b_{22} - b_{66})m^2n^2 + b_{12}(m^4 + n^4)$$

$$\bar{b}_{16} = (-2b_{11} + 2b_{12} + b_{66})m^3n + (2b_{22} - 2b_{12} - b_{66})mn^3$$

$$\bar{b}_{26} = (-2b_{11} + 2b_{12} + b_{66})n^3m + (b_{22} - 2b_{12} - b_{66})nm^3$$

$$\bar{b}_{66} = 2(2b_{11} - 4b_{12} + 2b_{22} - b_{66})m^2n^2 + b_{66}(m^4 + n^4)$$

where $m = \cos\alpha$, $n = \sin\alpha$ and b_{ij} are compliance constants of the composite along the principal axes. b_{ij} can be related to the mechanical constants of the material by

$$b_{11} = \frac{1}{E_{11}}\left(1 - \nu_{12}^2 \frac{E_{22}}{E_{11}}\right), \quad b_{22} = \frac{1}{E_{22}}(1 - \nu_{23}^2), \quad b_{12} = \frac{-\nu_{12}}{E_{11}}(1 + \nu_{23}), \quad b_{66} = 1/G_{12}$$

$$b_{44} = 1/G_{23}, \quad b_{55} = b_{66}$$

where E_{11} , E_{22} , G_{12} , G_{23} , ν_{12} , ν_{23} , and ρ are the mechanical properties of the composite and calculated using the following formulae

$$\rho = \rho_f V + \rho_m(1 - V), \quad E_{11} = E_f V + E_m(1 - V)$$

$$E_{22} = E_m \left[\frac{E_f + E_m + (E_f - E_m)V}{E_f + E_m - (E_f - E_m)V} \right]$$

$$\nu_{12} = \nu_f V + \nu_m(1 - V), \quad \nu_{23} = \nu_f V + \nu_m(1 - V) \left[\frac{1 + \nu_m - \nu_{12}E_m/E_{11}}{1 - \nu_m^2 + \nu_m \nu_{12}E_m/E_{11}} \right]$$

$$G_{12} = G_m \left[\frac{G_f + G_m + (G_f - G_m)V}{G_f + G_m - (G_f - G_m)V} \right], \quad G_{23} = \frac{E_{22}}{2(1 + \nu_{23})}$$

where indices m and f denote matrix and fibre, respectively. E , G , ν and ρ are the modulus of elasticity, the modulus of rigidity, the Poisson's ratio and the mass density, respectively.